Hunting reflections in Papua New Guinea: early processing results

David C. Henley and Han-Xing Lu

ABSTRACT

Papua New Guinea is among the most notoriously difficult areas in the world in which to acquire usable seismic reflection data. The rugged, forested terrain makes it very difficult to deploy both sources and sensors; and the complex near-surface layers contribute to serious coherent noise and statics on the resulting recorded seismic traces. Furthermore, the underlying geological structure is known to be complex, as well, adding to the difficulty of obtaining interpretable images. We show here some preliminary processing attempts, applied to a 2D-3C seismic line from Papua New Guinea, which may ultimately help to image reflections in these very challenging data.

INTRODUCTION

Operations reports for seismic surveys in Papua New Guinea often read more like adventure novels than factual accounts of the day-to-day operations of a high-tech corporation. The physical difficulties associated with deploying personnel and equipment in order to obtain usable seismic reflection images of PNG geology are well-known: rugged terrain covered with rain forest; few usable trails; torrential rain; and other physical hazards. In addition, it is often difficult to obtain good source/receiver coupling due to the relatively thin soil overlying harder rocks; and the underlying geological structures are complex, and would be hard to image even under good conditions. Processing data obtained under these conditions has proven to be as challenging as acquiring them in the first places.

Thanks to a new CREWES sponsor (Oil Search Ltd.), we have obtained a recent 2D seismic line from PNG. Our primary goal is to develop processing strategies for recovering reflection signal from the very noisy data. The line is a 3C line with 1880 dynamite shots spaced 30 m apart, shot into a split spread of 1070 receiver stations, receivers spaced 15 m, with nominal maximum offsets of +/- 6000 m. Ten seconds of 2 ms sampled data were recorded for the entire line; this 2D data set is a large one by CREWES standards. We focused first on the vertical component data, assuming that we would have the best chance of imaging those data.

Nothing demonstrates the difficulties with a particular data set as well as an example of the data themselves. Figure 1 shows a typical split-spread shot gather for the vertical component data from the PNG 3C-2D line, located about a third of the line length from the low numbered end of the line. We show only the first three seconds of data so that details can be more readily seen. It is evident from the pattern of first arrivals that the near-surface is complex and causes significant statics anomalies. It is very difficult to see any reflection-like events on this record (with only AGC and 8-12-40-50 bandpass filter applied); and even coherent noise patterns are disrupted by the statics.
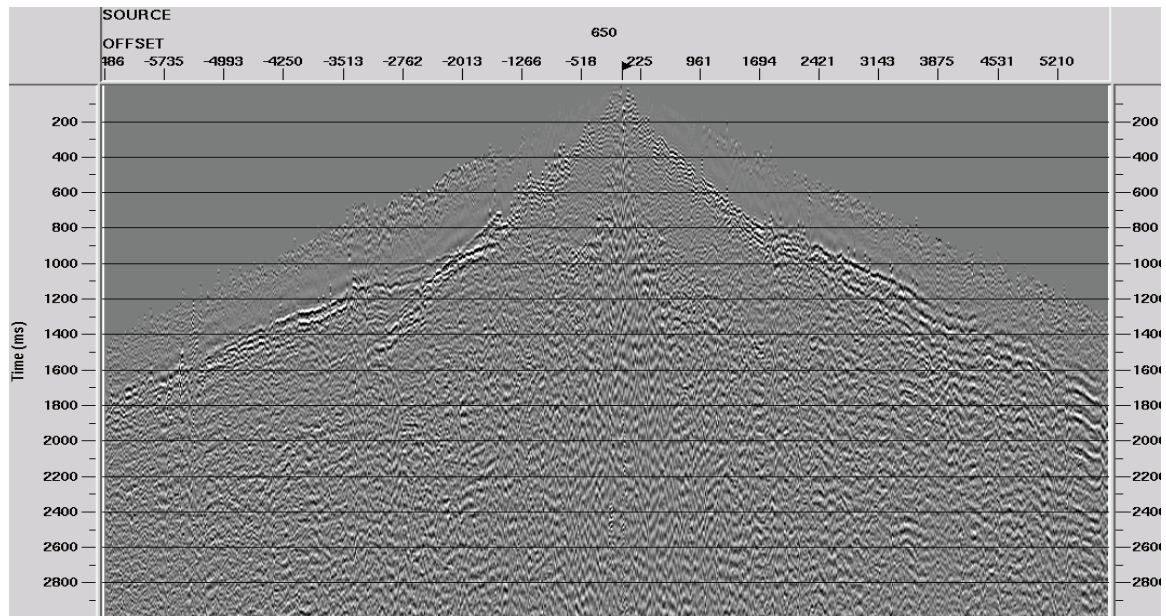
Typical PNG vertical component shot gather—AGC and bandpass only

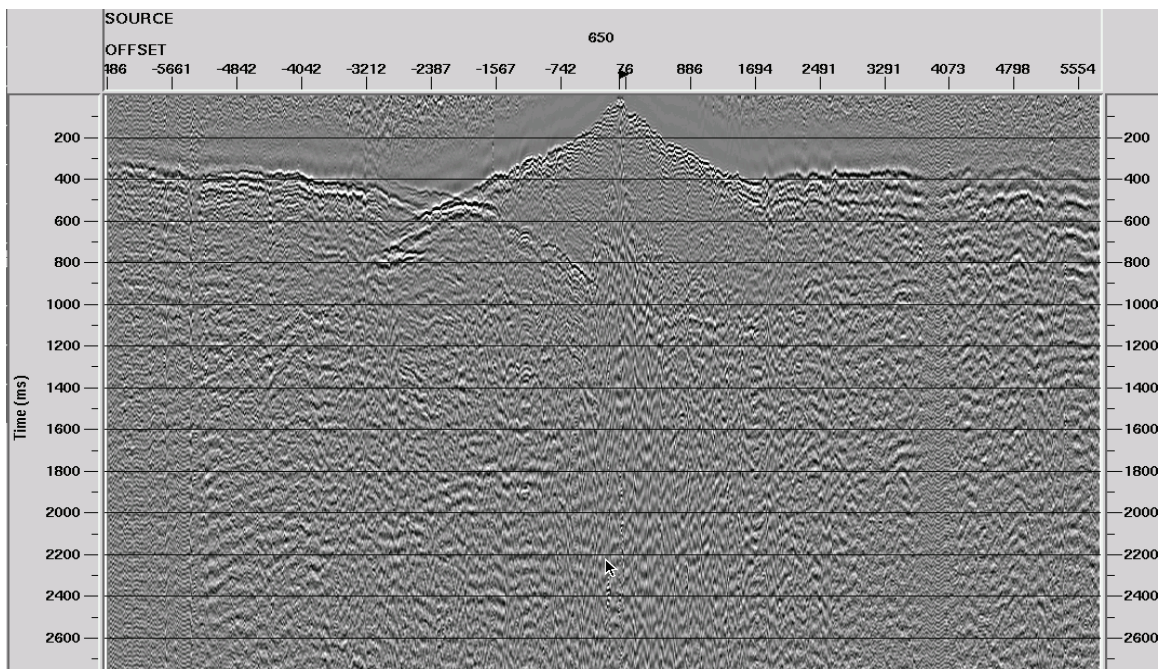FIG. 1. Typical PNG vertical component shot gather

PROCESSING STRATEGY

We decided to take a two-stage approach to the processing of these data. Initially, Han-Xing applied as much conventional processing as feasible, given the size of the data set and its poor quality, while D. Henley examined individual shot gathers to try to attenuate coherent noise and improve the signal bandwidth on the raw shots. When Han-Xing's processing efforts resulted in usable static corrections and an initial brute stack, D. Henley then processed the static-corrected shots to attenuate coherent noise and whiten the reflection signal. The result of this effort was a second brute stack, hopefully with improved reflection coherence. Below, we describe first the efforts to remove noise from and whiten raw shot gathers without the benefit of elevation or refraction statics; then we show the initial conventional processing and the resulting brute stack. Finally, we show the noise attenuation and whitening applied to the static-corrected shot gathers, then the stack of these 'improved' shot gathers.

Ordinarily, we begin processing raw shot gathers by applying rudimentary statics, such as elevation statics and refraction statics, to align direct arrivals and other source-generated coherent noises for more effective attenuation. Because of the size of this data set, and its poor quality, Han-Xing began this process by hand-picking direct arrivals on every sixth shot, and by flagging a large percentage of traces on the original gathers as bad traces, to be killed. Using the Hampson-Russell statics program GLI3D, she was able to improve the alignment and coherence of the arrival and refraction events on the vertical component shot gathers. Applying these statics, as well as elevation statics and a rudimentary stacking velocity function, Han-Xing managed to obtain a brute stack of these data, shown later in this report. Her static-corrected shot gathers were then provided to D. Henley for coherent noise attenuation and deconvolution (Henley, 2003a, 2003b), (Margrave et al. 2001), (Margrave et al. 2003).

In the meantime, as an experiment, working with the raw shot gathers, D. Henley attempted to attenuate coherent noise and deconvolve the data independently of any statics correction, using a brute-force technique described below. On these data he chose to artificially align direct arrivals and shallow refractions to assist with noise attenuation, then to remove this alignment after noise attenuation. The procedure is outlined in the steps below, based on ProMAX software (both standard modules and CREWES modules):

1. Apply linear moveout to the shot gathers to roughly align the first arrivals horizontally (4500 m/s velocity works relatively well). See Figure 2.

2. Apply two passes of 'Event alignment in window' and 'Header statics'. The event alignment module cross-correlates windowed portions of input traces (in this case, direct arrivals) with stacks of those traces to determine the time shift which best aligns each input trace with the stack. The maximum shift allowed, as well as the number of traces to include in the stack are critical parameters for this process. Since the possible shifts in the first arrivals of the shot record are so large, we used 100 ms; and since we want the first arrivals aligned as smoothly as possible, we used a large number of traces for the stack (200 for the first pass, 100 for the second). The module 'Header statics' applies the 'tot_alin' trace header static, created by the 'Event alignment in window' process to each trace, in order to align it with its neighbours. See Figure 3.

3. Remove the previously applied linear moveout, as in Figure 4.

PNG shot gather with 4500 m/s linear moveout applied

FIG. 2. PNG vertical component shot gather from Figure 1 with linear moveout applied to partially align coherent first arrival events and shallow refractions.
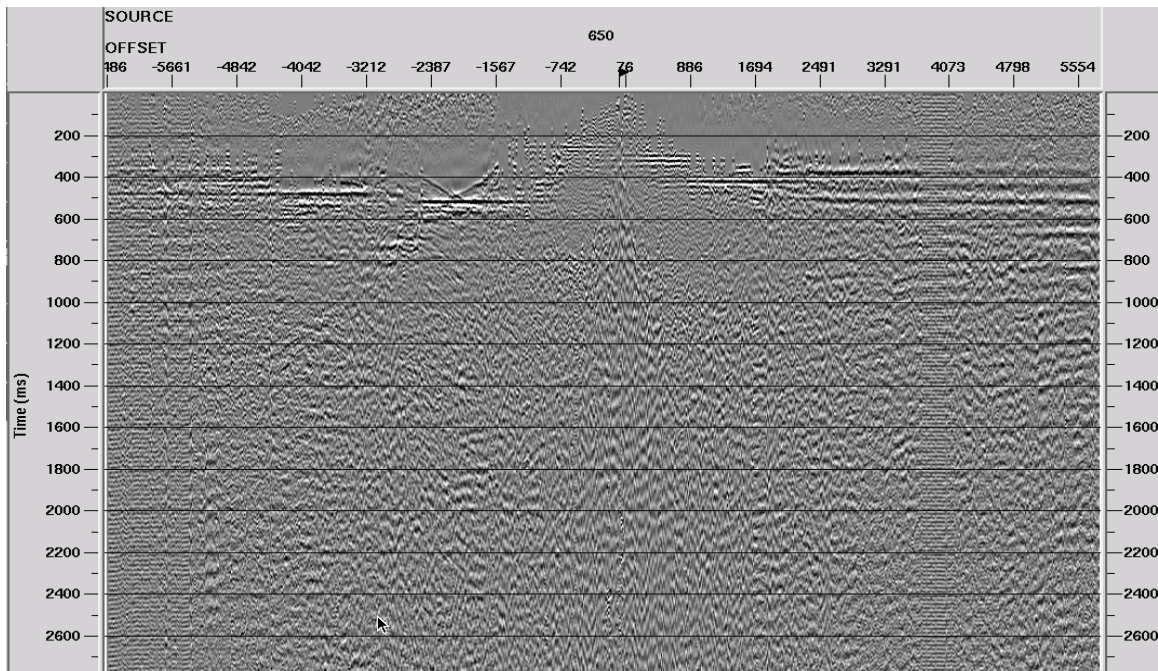
PNG shot gather with 4500 m/s linear moveout applied, coherent energy forced to align

FIG. 3. PNG vertical component shot gather after alignment of shallow coherent arrival energy.
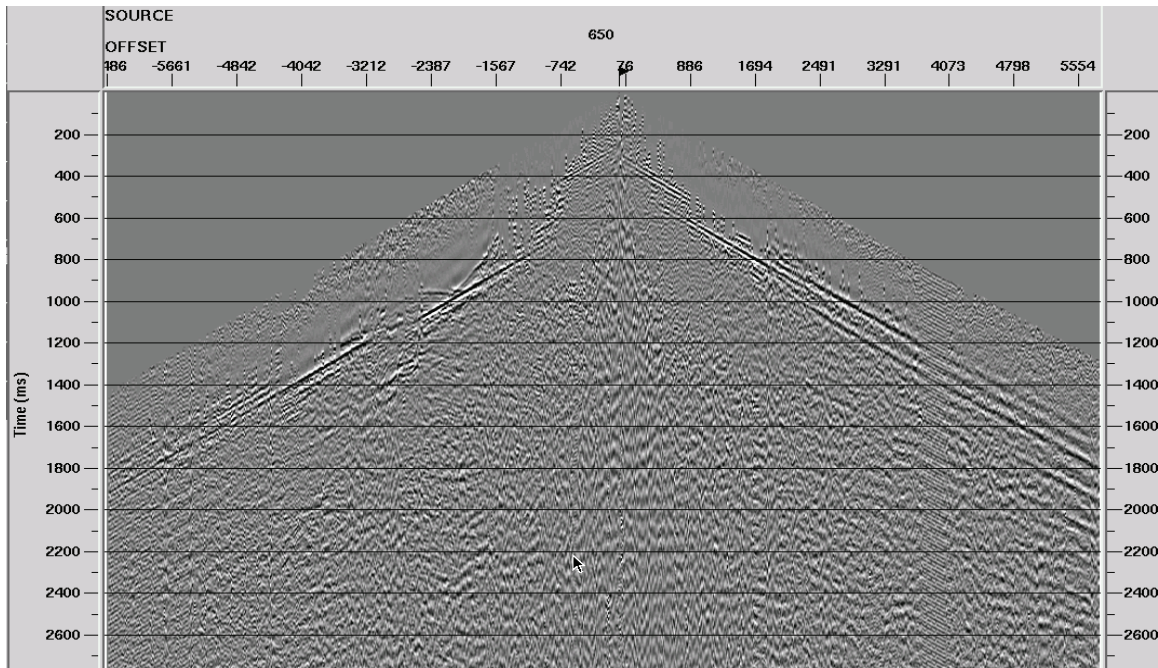

PNG shot gather with coherent energy aligned, linear moveout removed

FIG. 4. PNG vertical component shot gather after coherent event alignment, ready for radial trace filtering to attenuate coherent noise.

   4. Apply radial trace fan filter using the CREWES ProMAX module 'Radial filter'

5. Examine filtered gathers for residual linear noises.

6. Apply radial trace dip filters in pairs (+/- dip velocity) for detected linear noises and their aliases (In this case, 3000 m/s, 1500 m/s, and 750 m/s)

7. Remove the 'tot_alin' static from each trace.

8. Re-apply the linear moveout.

9. Apply Gabor deconvolution in the single trace mode to whiten the spectrum.

10. Remove the linear moveout.
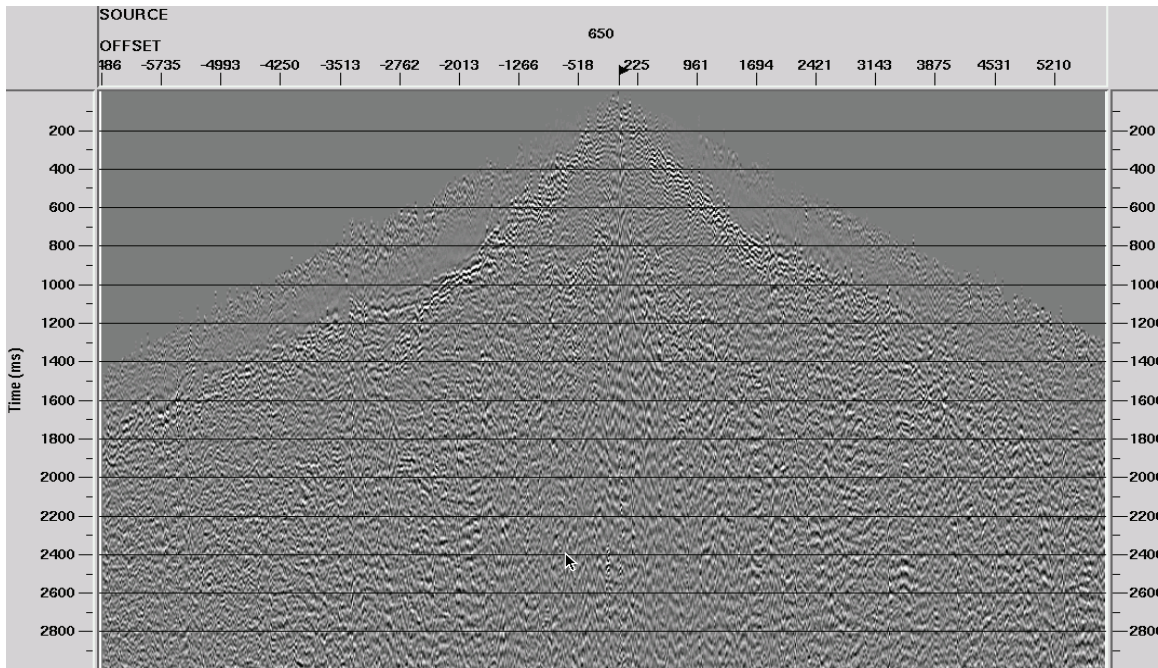
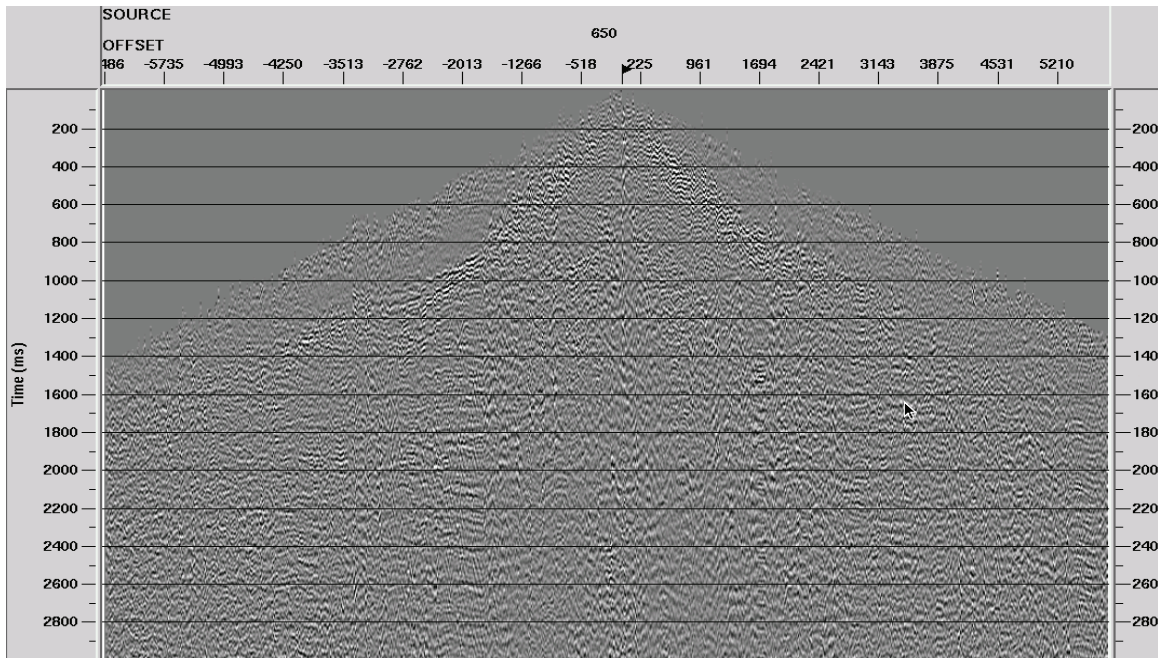

PNG shot gather with 1 pass radial filter—fan filter mode

FIG. 5. PNG vertical component shot gather after first pass of radial trace filtering—fan filter mode.

Figure 5 shows the same shot gather as Figure 1 after the first pass of radial trace filtering.
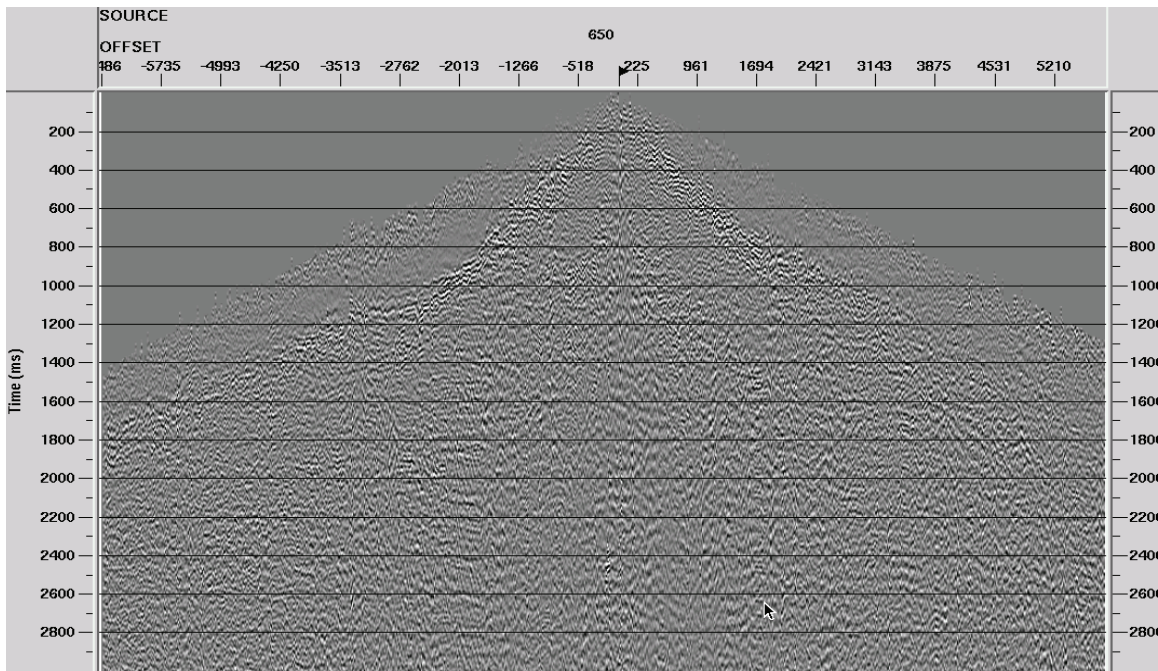
PNG shot gather with 1 pass radial filter—fan filter mode—2 radial dip filters +/- 3000 m/s

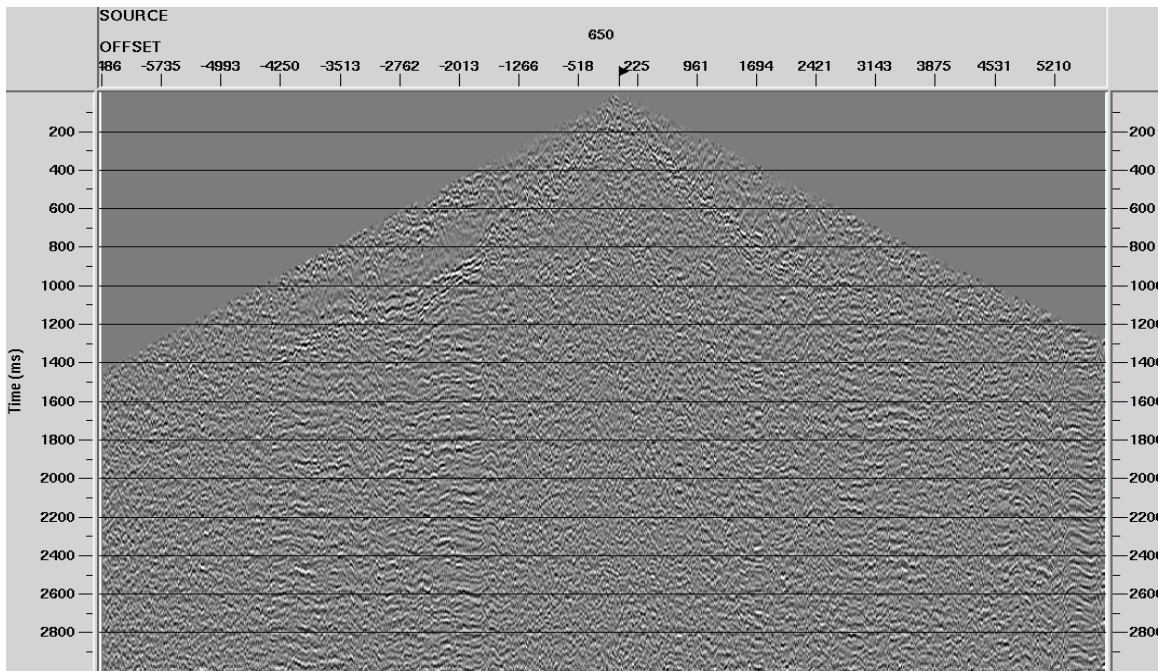FIG. 6. PNG vertical component shot gather after 2 radial trace filter passes.

PNG shot gather with 1 pass radial filter—fan filter mode—2 radial dip filters +/- 3000 m/s, 2 dip filters +/- 1500 m/s

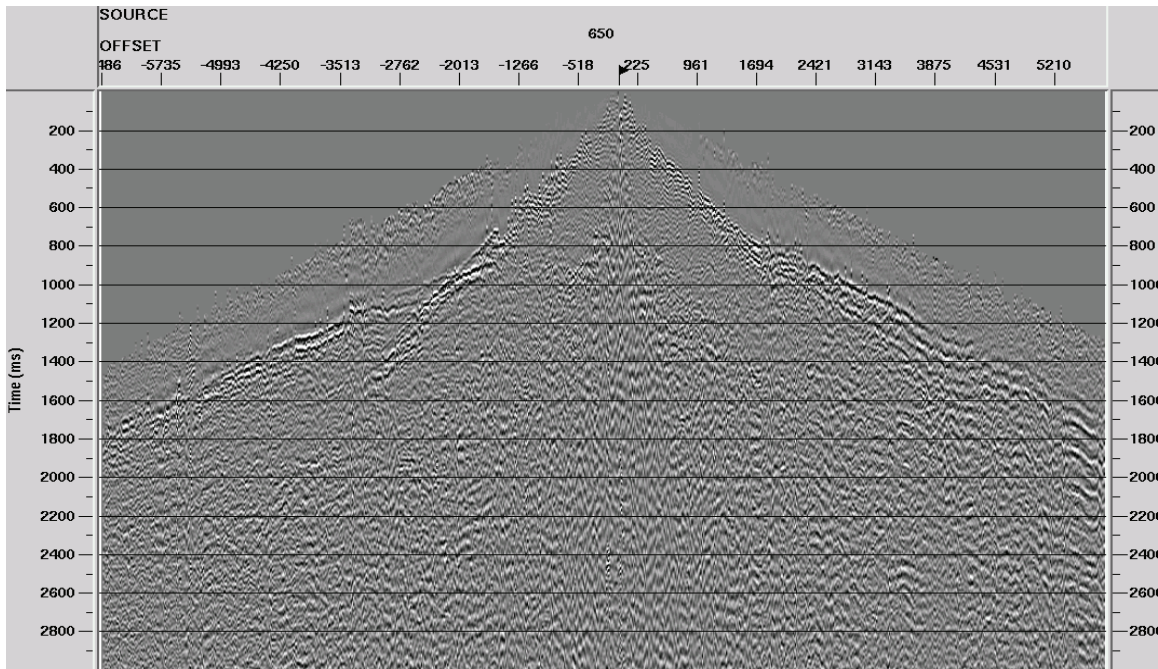FIG. 7. PNG vertical component shot gather after 3 radial trace filter passes.
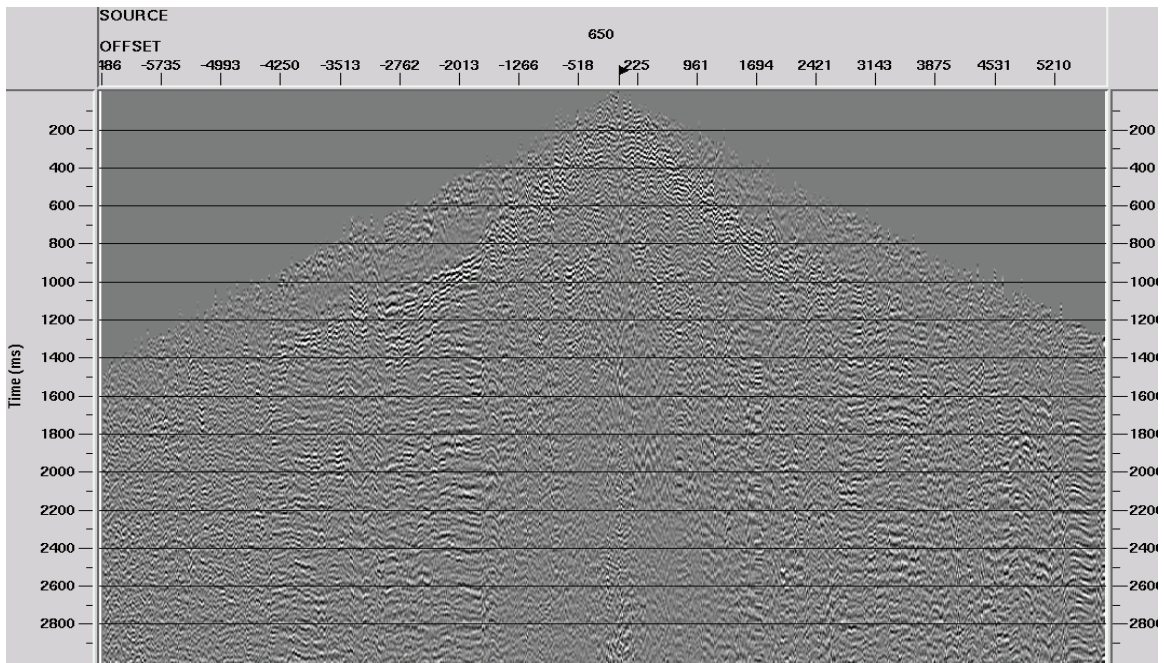
PNG shot gather with 1 pass radial filter—fan filter mode—2 radial dip filters +/- 3000 m/s, 2 dip filters +/- 1500 m/s, 2 dip filters +/- 750 m/s

FIG. 8. PNG vertical component shot gather after 4 radial trace filter passes.

PNG shot gather with 1 pass radial filter—fan filter mode—2 radial dip filters +/- 3000 m/s, 2 dip filters +/- 1500 m/s, 2 dip filters +/- 750 m/s, Gabor deconvolution

FIG. 9. PNG vertical component shot gather after radial trace filtering and Gabor deconvolution.


PNG shot gather—AGC and bandpass only

FIG. 10. PNG vertical component shot gather—raw record for comparison to Figure 9.

Figures 6, 7 and 8 show the same gather after each subsequent pass of dip filtering. Progressive improvement can be seen on each figure. Segments of events that are probably reflections can now be seen at various places on the gather (see arrows). The

final result in Figure 9 shows the effect of Gabor deconvolution on the filtered shot gather (mostly amplitude adjustment and slight broadening of event bandwidth). Figure 10 shows the original raw shot gather for comparison.

These modest results have not at present been further processed by removing statics and stacking. In the near future, we hope to revisit the above technique, but with known elevation and refraction statics applied, prior to forcing the coherent event alignment.

Instead, the shot gathers processed by Han-Xing were subjected to several passes of radial trace filtering, after application of statics, and deconvolved with Gabor deconvolution. To indicate the severity of the statics problem, Figure 11 is a plot of station elevations along the line. Note that the total relief is around 1000 m. The statics that result just from elevations are shown in Figure 12. A partially successful attempt to use the GLI3D program to derive refraction statics resulted in the statics displayed in figures 13 and 14. An example shot gather before statics application appears in Figure 15, while the same gather after statics application appears in Figure 16. Subsequent coherent noise attenuation and deconvolution yield the gather shown in Figure 17.
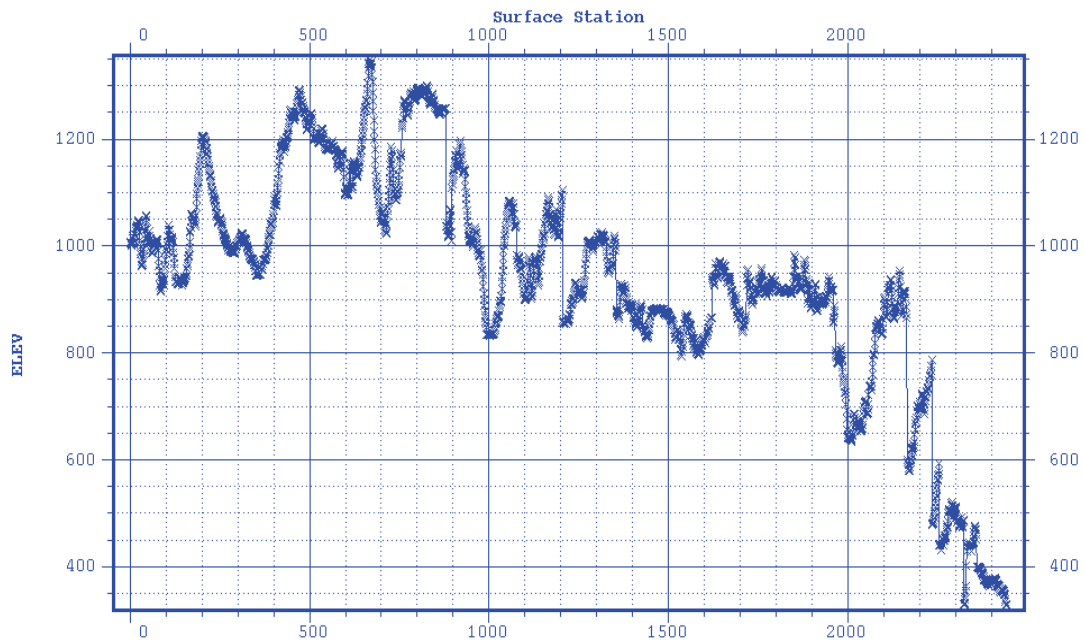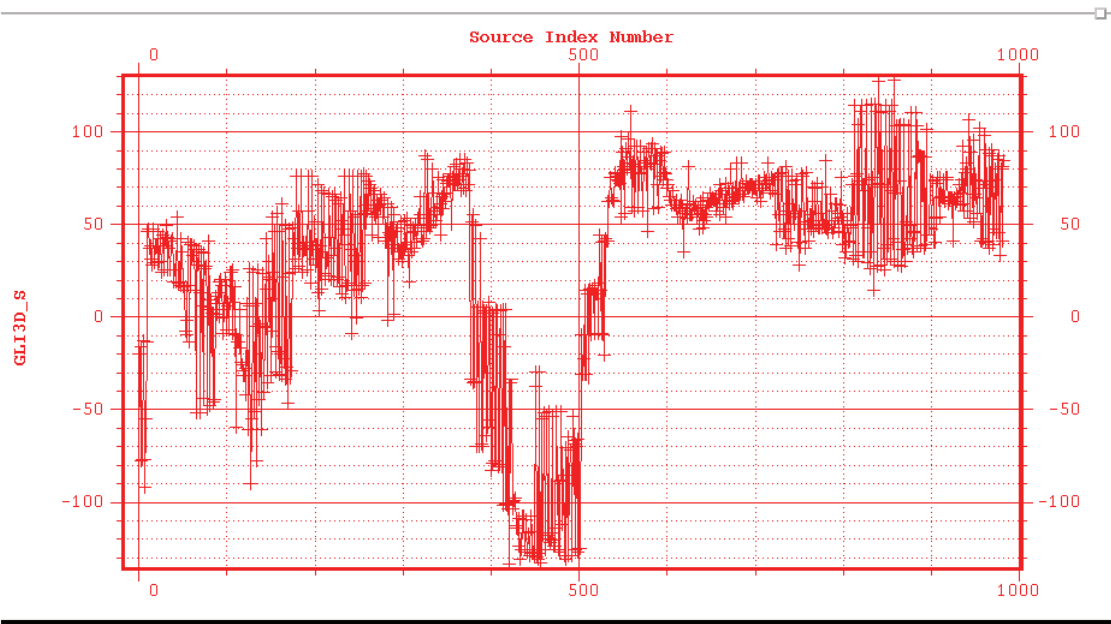

The elevations of the survey stations, there is about 1000m relief.

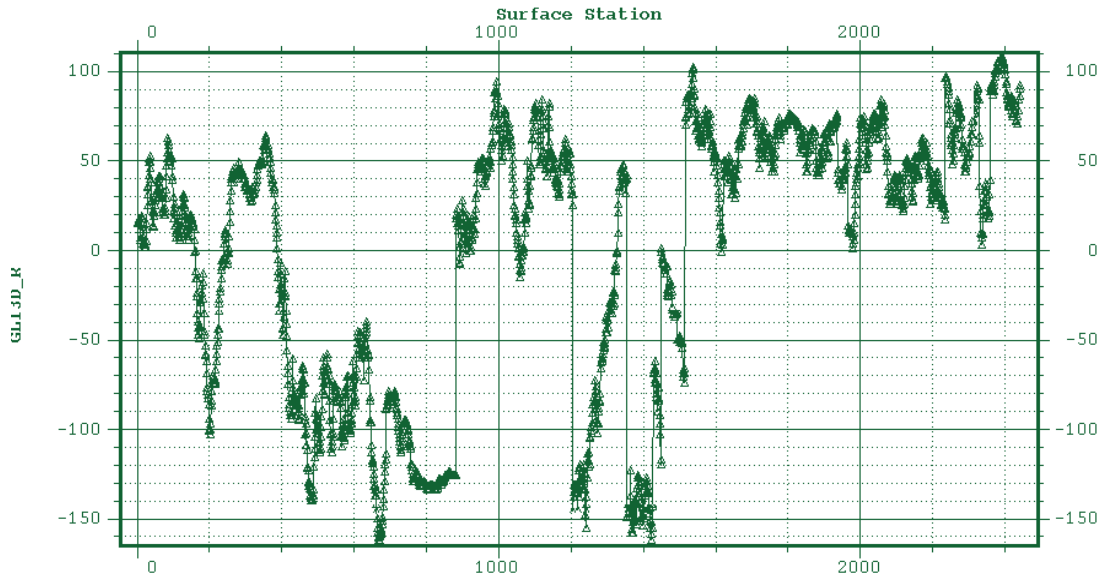FIG. 11. Station elevations along the PNG 3C line.
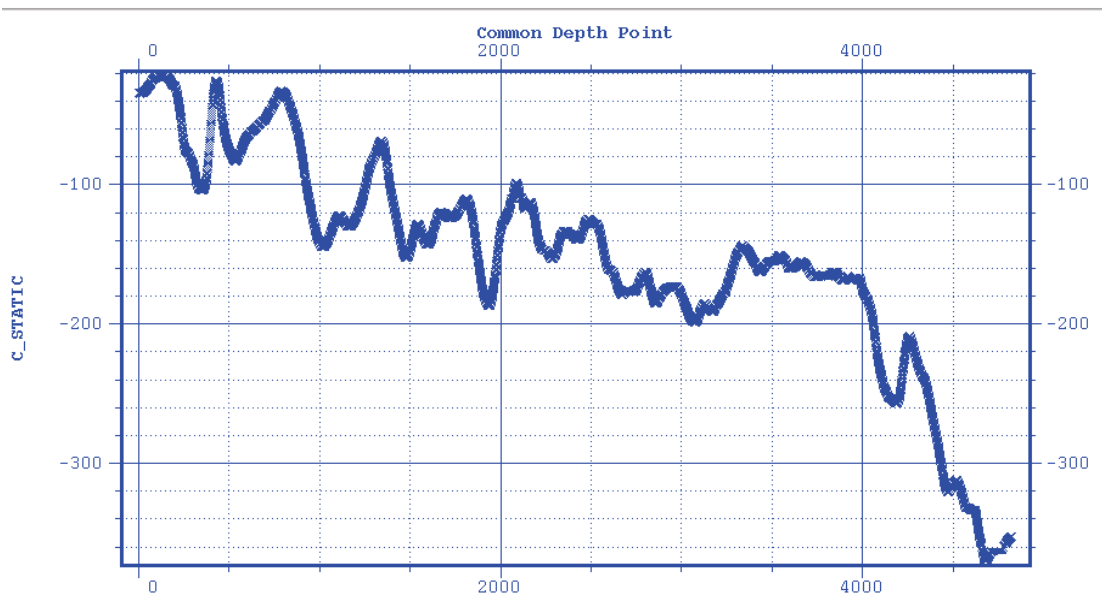
Elevation statics, weathering V=1400m/s, replacement V=5400m/s

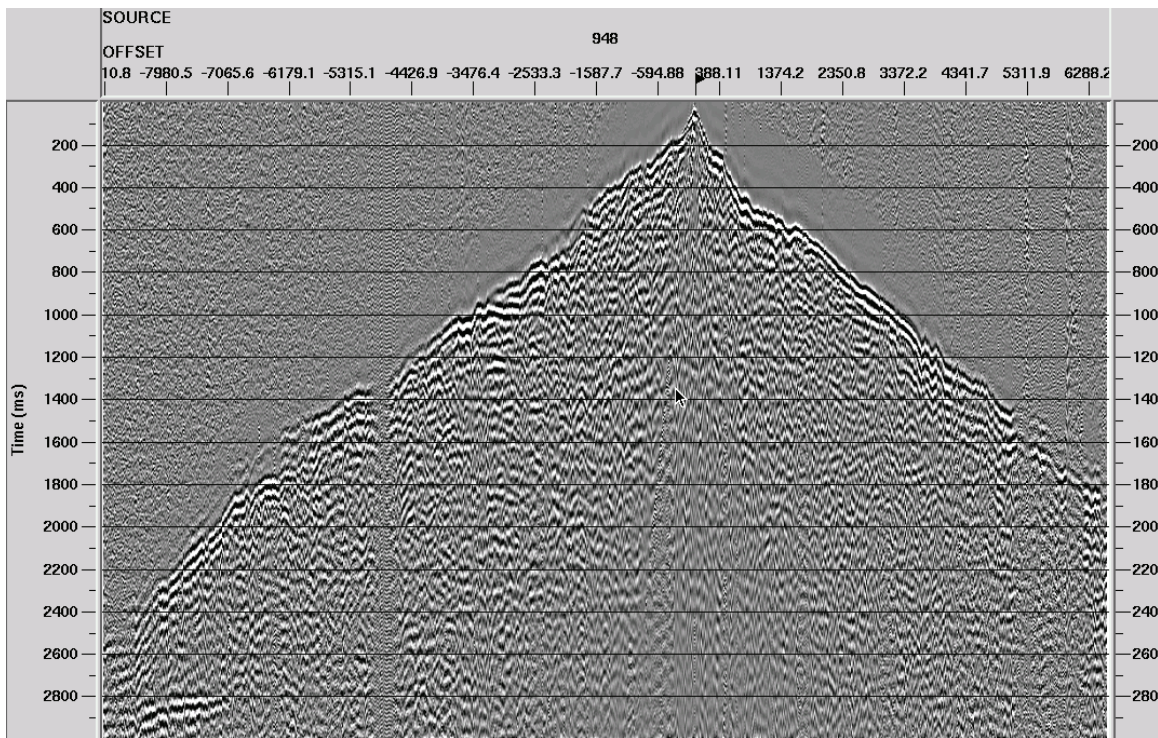FIG. 12. The statics required to correct for the elevation differences in Figure 11.

Refraction statics for sources.

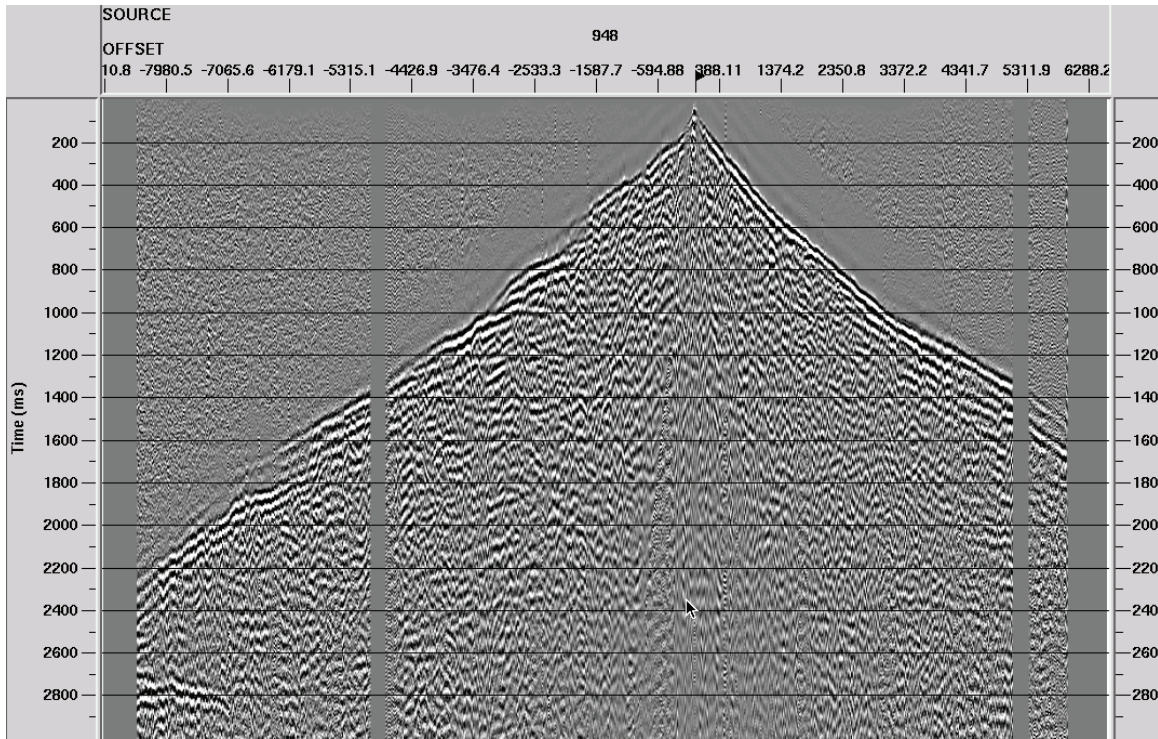FIG. 13. Source refraction statics from GLI3D

Refraction statics for receivers.

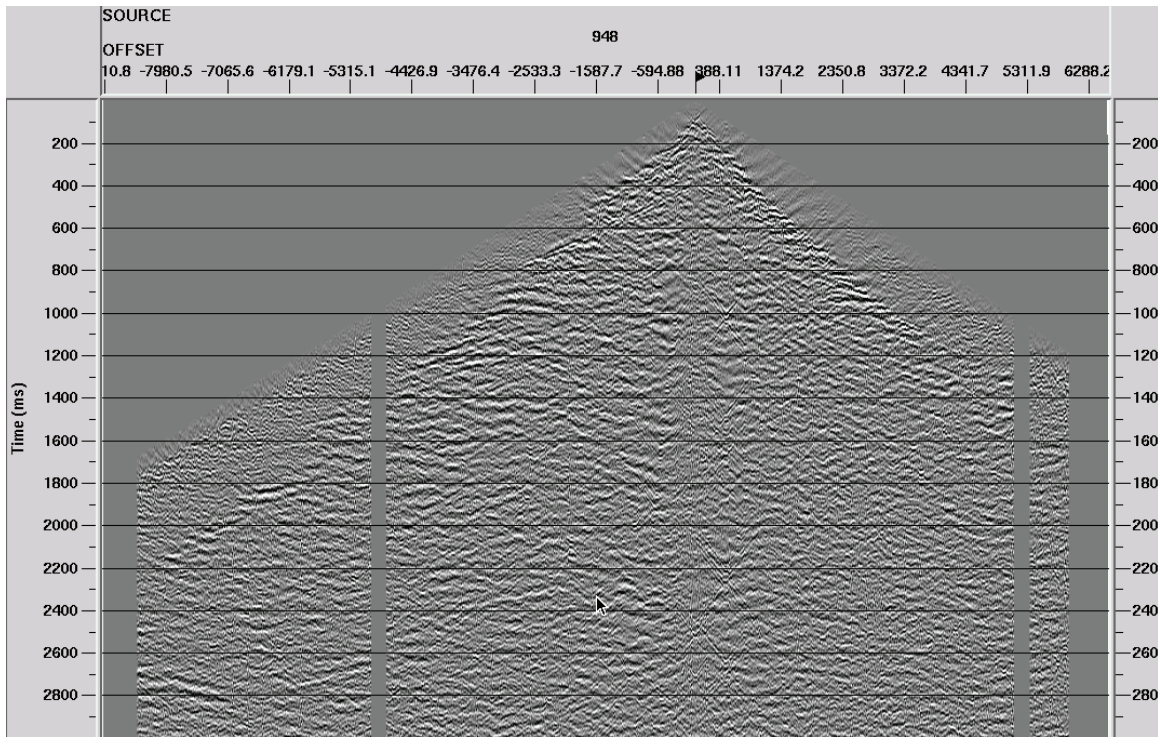FIG. 14. Receiver refraction statics from GLI3D

Shot 948 raw

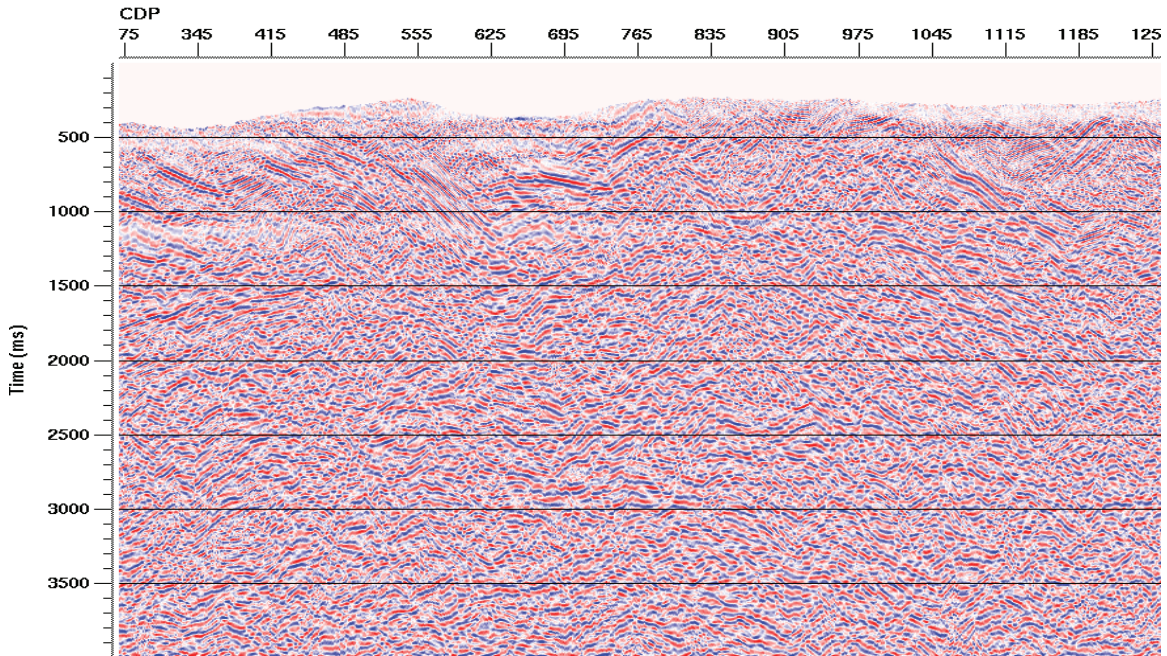FIG. 15. Raw shot gather for source position 948

Shot 948 after statics

FIG. 16. Raw shot gather with elevation and refraction statics applied, for source position 948
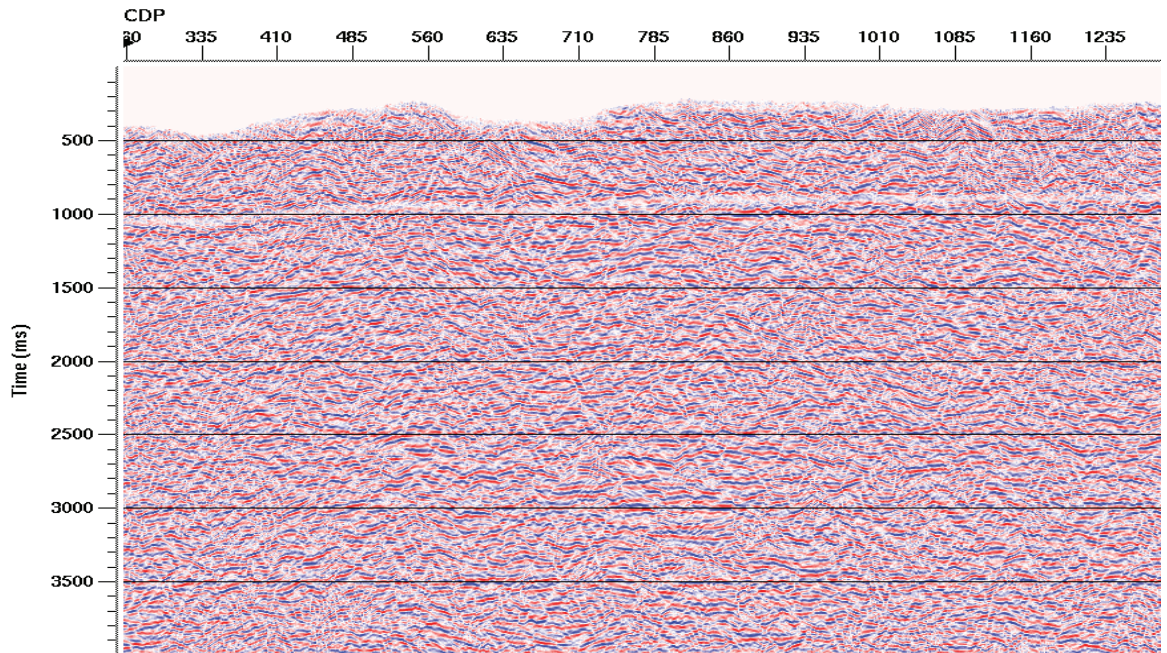

Shot 948 after statics, coherent noise attenuation, Gabor deconvolution

FIG. 17. Shot gather 948 after coherent noise attenuation and Gabor deconvolution.

A portion of PNG line after brute processing, no noise filtering or decon

FIG. 18. Brute stack of PNG vertical component for a portion of the line, with only elevation statics and refraction statics applied. The image artefact at 1000 ms is unexplained at this time.

Stack of PNG vertical component data after coherent noise attenuation and Gabor deconvolution

FIG. 19. Stack of PNG vertical component with coherent noise attenuation and Gabor deconvolution applied pre-stack. The image artefact at 1000 ms is unexplained at this time.

We show, finally, the results of stacking the heavily edited vertical component PNG data after applying only elevation statics and refraction statics (Han-Xing's initial brute stack), in Figure 18. The display represents only a portion of the line. Figure 19 shows the same line segment, but after the gathers have been additionally subjected to coherent noise attenuation and Gabor deconvolution.

DISCUSSION

As can be seen by comparing Figures 18 and 19, there are considerable differences in the events. Most notably, the shallow, steeply dipping events so apparent on the unfiltered result are mostly missing from the filtered result, leading to the conjecture that these events are refractions rather than reflections. During the filtering, direct arrivals and shallow refractions were strongly attenuated, as were dipping events with apparent velocity less than 2000 m/s. Thus, legitimate reflection segments with low velocities may have been attenuated, as well.

The results presented here are very early and by no means represent the final product. We hope to try a number of different approaches as we re-examine these challenging data in the coming months. Since the gathers filtered and deconvolved using forced alignment of coherent energy seem to have more coherent 'reflection-like' events and greater bandwidth (Figure 9) than those with only elevation and refraction statics applied (Figure 17), we hope to apply both known statics and artificial alignment to improve coherent noise attenuation. We also need to examine coherent events carefully to ensure that we're not filtering out steeply dipping reflections that fall within the velocity apertures of our filters.

ACKNOWLEDGEMENTS

REFERENCES

Henley, David C. 2003, Coherent noise attenuation in the radial trace domain, Geophysics, **68**, No. 4, pp1408-1416, 2003.

Henley, D.C., 2003, More coherent noise attenuation in the radial trace domain, CREWES 2003 research report **15**.

Margrave, G.F., and Lamoureux, M.P., 2001, Gabor deconvolution: CREWES 2001 research report, **13**.

Margrave, G.F., Linping Dong, Grossman, J.P., Henley, D.C., and Lamoureux, M.P., 2003, Gabor deconvolution: extending Wiener's method to nonstationarity: CREWES 2003 research report, **15**.